Core-hole effects on theoretical electron-energy-loss near-edge structure and near edge x-ray absorption fine structure of MgO

AUTHOR(S):

Mizoguchi, T; Tanaka, I; Yoshiya, M; Oba, F; Ogasawara, K; Adachi, H

CITATION:

Mizoguchi, T ...[et al]. Core-hole effects on theoretical electron-energy-loss near-edge structure and near edge x-ray absorption fine structure of MgO. PHYSICAL REVIEW B 2000, 61(3): 2180-2187

ISSUE DATE:

2000-01-15

URL:

http://hdl.handle.net/2433/39838

PHYSICAL REVIEW B VOLUME 61, NUMBER 3 15 JANUARY 2000-I

Core-hole effects on theoretical electron-energy-loss near-edge structure and near-edge x-ray absorption fine structure of MgO

Teruyasu Mizoguchi
Department of Materials Science and Engineering, Kyoto University, Sakyo, Kyoto 606-8501 Japan

Isao Tanaka
Department of Energy Science and Technology, Kyoto University, Sakyo, Kyoto 606-8501, Japan

Masato Yoshiya, Fumiyasu Oba, Kazuyoshi Ogasawara, and Hirohiko Adachi
Department of Materials Science and Engineering, Kyoto University, Sakyo, Kyoto 606-8501 Japan

(Received 11 January 1999; revised manuscript receipt 9 July 1999)

First-principles molecular orbital calculations using model clusters are made in order to reproduce and interpret experimental electron-energy-loss near-edge structure and near-edge x-ray absorption fine structure of MgO at Mg *K*, $L_{2,3}$ and O *K* edges. Ground-state calculations using a model cluster composed of 125 atoms and by a band-structure method are in good agreement, but they do not reproduce the experimental spectra satisfactory. They are well reproduced only by the cluster calculations for the Slater transition state, where a half-electron is removed from a core orbital and placed into the lowest unoccupied molecular orbital. The core-hole effect is therefore essential for theoretical reproduction of the spectral shapes. A large supercell is required to reproduce the experimental spectra when one uses a band-structure method. The origin of peaks appearing in the experimental spectra is interpreted in terms of orbital interactions using overlap-population diagrams. Some features of the spectra at different edges are pointed out to have common origins. Experimental spectra are aligned accordingly. The transition energies and qualitative features of experimental spectra are found to be reproduced even using a smaller cluster composed of 27 atoms, although some of fine structure is missing.

I. INTRODUCTION

An electron-energy-loss spectrometer (EELS) is often equipped in modern transmission electron microscopes (TEM's), which constitutes a nanoscale probe that is very useful in solid-state physics and chemistry as well as materials science. The structure within approximately 20 eV from the core-loss edge is usually referred to as the electron-energy-loss near-edge structure (ELNES), which is analogous to the near-edge x-ray absorption fine structure (NEXAFS), that is, a synonym of x-ray absorption near-edge structure (XANES). On the core-loss process, an electron is excited from a core level to an unoccupied state by a electric dipole transition. As a result, experimental ELNES and NEXAFS are related to the unoccupied partial density of states of the selected atom that is allowed by the electric dipole selection rule.

Efforts to reproduce ELNES and NEXAFS by first-principles calculations are not always successful even today. Literature from the early days can be found in Ref. 1. The reasons for the disagreement between theoretical spectra and experimental spectra may be twofold: (1) Even when local-density approximation (LDA) calculations are made from first principles, results of unoccupied density of states sometimes show a stronger dependence on the choice of the basis functions as compared with the occupied states especially at high energies. Theoretical spectra in early literature sometimes differ from those by some more sophisticated methods. (2) Most theoretical calculations that have been used to compare the experimental spectra were done for the ground state. In other words, the presence of a core hole has been completely ignored. In absorption phenomenon, an electron is excited from a core level to an unoccupied orbital, leaving a core hole. The unoccupied band structure is, in general, changed by the presence of the core hole. The calculation for the ground state reproduces the experimental spectrum only when the core-hole effect is not significant.

First-principles cluster calculations on the basis of molecular orbital (MO) theory within the one-electron approximation have been successful for reproduction of ELNES of some oxides.[2–6] Core-hole effects can be included in the self-consistent calculations, which were pointed out to be essential for the ELNES calculations.[4–6] Since the excited electron is localized near the core hole, cluster calculations should be advantageous for the ELNES reproduction compared with band-structure methods unless a sufficiently large supercell is chosen. Very recently, the present authors have reported the effects of a core hole in the unoccupied density of states using model clusters of hexagonal boron nitride.[7] Wave functions are found to localize significantly near the core hole, thereby changing their energies as well as spatial distribution. They are very different from the Bloch states assumed in a band-structure calculation on the basis of a structural unit cell. When the presence of the core hole is ignored, in other words at the ground state, small clusters exhibit better agreement with the experiment as compared with large clusters because wave functions are made to localize in small clusters.

In the present study, we calculate the unoccupied density of states of MgO systematically including core holes in Mg

$1s$ (Mg K edge), Mg $2p$ (Mg L_{23} edge) and O $1s$ (O K edge). Preliminary results were already published in Ref. 2. However, the core hole was not included in that work. Assignments for spectral features have not been given, either. We aimed at a more precise calculation under the same methodology and understanding of the origin of each peak that appears in the ELNES. MgO is chosen because it is one of the standard systems that has often been investigated both by experiments and theories. Experimental spectra by ELNES and NEXAFS thus far reported were all in good agreement. Moreover, the authors are aware of a very recent work to reproduce ELNES of MgO at the three edges by a mixed-basis pseudopotential approach.[8] It would be very interesting to compare theoretical results by different methods.

II. COMPUTATIONAL PROCEDURE

MgO shows a rocksalt structure with a lattice constant of 421.2 pm. First-principles molecular-orbital (MO) calculations were made for MgO using model clusters composed of 125 atoms. The excited atom for the corresponding core loss was put at the center of the clusters. Model clusters were embedded in point charges located at the external atomic sites to produce an effective Madelung potential. The program SCAT,[9] based on the discrete variational $X\alpha$ (DV-$X\alpha$) method,[10] was employed in which numerical atomic orbitals (NAO) were used as basis functions. They were generated flexibly by solving the radial part Schrödinger equation for a given environment. Minimal basis sets were used in order to clarify the simple relationship between spectral features and chemical bondings. Basis sets are $1s$, $2s$, and $2p$ for O and $1s$, $2s$, $2p$, $3s$, $3p$, and $3d$ for Mg.

The partial density of states (PDOS) for the ith atomic orbital $N_i(E)$ is given by

$$N_i(E)=\sum_l Q_i^l G_l(E-\varepsilon_l), \tag{1}$$

where $G_l(E\text{-}\varepsilon_l)$ is a Gaussian function of 1.0 eV full width at half maximum (FWHM), ε_l is the MO eigenvalue, and Q_i^l is provided by

$$Q_i^l=\sum_j Q_{ij}^l . \tag{2}$$

Q_{ij}^l is the overlap population between ith and jth atomic orbitals as defined by

$$Q_{ij}^l=C_{il}C_{jl}S_{ij} , \tag{3}$$

where S_{ij} is the overlap integral given by

$$\int \chi_i^*(\mathbf{r})\chi_j(\mathbf{r})d\mathbf{r}=S_{ij} . \tag{4}$$

χ_i and C_{il} are the ith atomic orbital and its coefficient for the lth MO, respectively.

The photoabsorption cross section (PACS) is proportional to the oscillator strength for the transition for photon absorption between the ith core state and lth MO, which is given by

$$I_{i\rightarrow l}\propto \Delta E|\langle l|\mathbf{r}|i\rangle|, \tag{5}$$

where ΔE represents the transition energy. The value was obtained directly by the numerical integration of the dipole matrix. The PACS was also broadened by Gaussian functions of 1.0 eV FWHM.

In the electron-energy-loss process, an electron is promoted from a core level to an unoccupied state, leaving a core hole. As a result, the electronic structure at this state differs from that of the ground state. In order to reproduce the experimental spectrum, self-consistent calculations should be carried out including a core hole. In the present study, calculations were made for both the ground state and Slater's transition state,[11] where half of an electron is removed from a core orbital to put it into the lowest unoccupied MO. The calculation for Slater's transition state is a useful way to compute the difference in total energies between initial and final states, i.e., the absolute transition energy. However, it does not mean that the core-hole effects to change the energies and spatial distribution of wave functions are best reproduced by the calculation for the transition state. It is true that the influence of the core hole has been estimated mainly by increasing the atomic number of the nucleus undergoing excitation by 1, which is called the $Z+1$ approximation[12] or final-state approximation. We have systematically calculated the unoccupied MO by three states, namely ground, final, and Slater's transition states in some systems,[4,7] and found that the final-state calculations are often too extreme to reproduce the experimental spectrum. In the present study, we will therefore mainly compare results of Slater's transition state with those of the ground state.

III. RESULTS AND DISCUSSION

A. Mg *K*-edge spectrum

Figure 1 displays experimental ELNES by Lindner *et al.*[13] in comparison with three theoretical spectra by cluster calculations and full potential linearized augmented plane wave (FLAPW).[14] Cluster calculations were made using the $(Mg_{63}O_{62})^{2+}$ cluster for both the ground state and Slater's transition state where a half electron was removed from a Mg $1s$ orbital of the central Mg atom of the cluster to be put into the lowest unoccupied molecular orbital. The temporary spin polarization associated with the transition was taken into account. The electric dipole selection rule allows a transition from Mg $1s$ to unoccupied p-orbitals. Since we use minimal basis functions for the present calculation in order to clarify the simple relationship between spectral features and chemical bondings, only the Mg $3p$ component at the core-hole Mg atom is of interest. Both the PDOS and the PACS that is proportional to the oscillator strength were computed. Although the PDOS and PACS differ in intensity, spectral features agree satisfactory. In other words, the PACS is well approximated by the corresponding PDOS. This can be ascribed to the use of ''optimized'' numerical atomic orbitals. We will hereafter show only the PDOS for simplicity.

The experimental spectrum and the PDOS for the transition-state calculation are labeled by letters. The origin of each peak will be shown afterward in the present paper. The experimental spectrum and the PDOS for the transition-state calculation are aligned so as to make best matches. The error in the absolute transition energy is 7 eV, which is approximately 0.5% of the absolute transition energy. Other

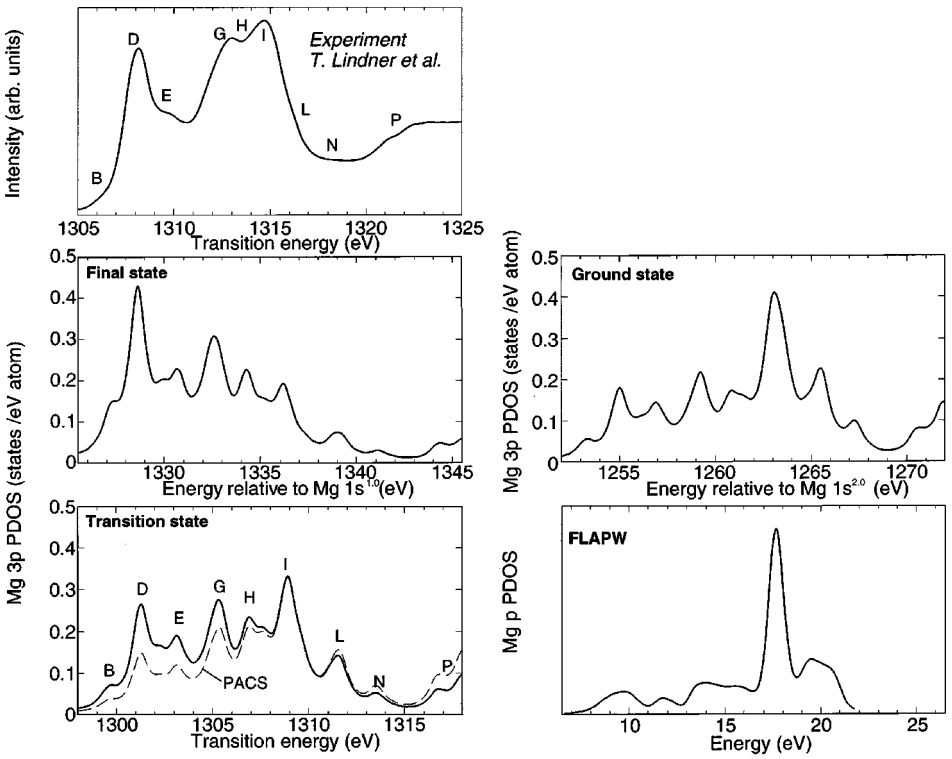

FIG. 1. (Left: from top to bottom) Experimental Mg *K*-edge ELNES of MgO by Lindner *et al.* (Ref. 13). Theoretical Mg 3*p* PDOS by a cluster $(Mg_{63}O_{63})^{2+}$ calculated for the final state and Slater's transition state. (Right: from top to bottom) Theoretical Mg 3*p* PDOS for the ground state. Mg *p* PDOS by the FLAPW band-structure calculation. The energy by the FLAPW was shifted so as to make the highest occupied band to be zero.

than the absolute transition energy, spectral features in the first 10 eV are fairly reproduced. Although peak *B* is not clearly visible in the experimental spectrum, we can assume its presence because of a change in curvature at the lower-energy tail of peak *D*. The shapes in the energy region *G* to *I* and above peak *I* do not agree well. Yet, it is in much better agreement than the theoretical results by the two other methods as shown in Fig. 1.

The FLAPW calculation was made for a rhombohedral primitive cell composed of two atoms. We can see a pronounced feature at around 17 eV from the highest occupied band. Result of the *p* projected density of states by a mixed-basis pseudopotential calculation by Köstlmeier and Elsässer[8] using the same unit cell is almost the same as the FLAPW result. These band-structure calculations were made for the ground state. Our ground-state calculation using the cluster composed of 125 atoms shows a similar pronounced feature although the relative peak height of the strongest peak is approximately halved. The relative intensity is halved again when a half-filled core hole is introduced into the same cluster. These results imply that wave functions are significantly localized from the Bloch states to show the features that appear in the experimental ELNES. Even the cluster calculation for the ground state makes the wave function somehow localize compared with the band-structure calculation for the ground state. In order to reproduce the experimental ELNES, it is necessary to include the core-hole effect. In addition to the ground-state calculations, Köstlmeier and Elsässer[8] included the effect of the core hole using special pseudopotentials made for the core-hole states. However, they did not found significant improvement regarding the reproduction of the ELNES. They found again a single pronounced peak rather than the multipeak feature, although a notable energy shift due to the inclusion of the core hole is found. They made a further trial to calculate the DOS using a supercell composed of eight atoms. It did not improve the result significantly, either. As will be discussed afterward, the reproduction of the localized states by band-structure calculation may require a much larger supercell, which is a very demanding calculation even today.

The calculated spectrum for the final state is shown for comparison in Fig. 1. The peak that corresponds to peak *D* in the experimental spectrum is markedly pronounced at the final state, although peak positions are not significantly altered by the presence of the core hole. At the present moment, the calculation at the final state seems to be too extreme to take account of the core-hole effect into the cluster calculation of this size.

B. Mg $L_{2,3}$-edge spectrum

An experimental ELNES spectrum by Lindner *et al.*[13] is shown in Fig. 2 (top). It should be noted that peak *A* in the corresponding NEXAFS spectrum by O'Brien *et al.*[15] is much stronger. The sum of Mg 3*s* and 3*d* PDOS's obtained by the same cluster as used in Fig. 1 is compared with the experimental spectrum. The L_{23}-edge PACS was computed and compared in the same figure. The PACS is found to be well approximated by the sum of PDOS's, which means that the contributions of the Mg 3*s* and 3*d* components to the L_{23}-edge PACS are almost the same. We got similar results for the L_{23}-edge PACS for metal oxides with third-row elements, such as SiO_2 (Ref. 5) and α-Al_2O_3 (Ref. 4). This may be contrasted with the conclusion in literature regarding the relative contributions of *nd* and $(n+1)s$ orbitals to the L_{23}-edge NEXAFS (Refs. 16 and 17) of heavier atoms. They have reported that the transitions to *s* states is negligible as compared to the transition to the *d* states. But, we should emphasize that we are dealing with 3*s* and 3*d* orbitals having the same principal quantum number. The spatial distri-

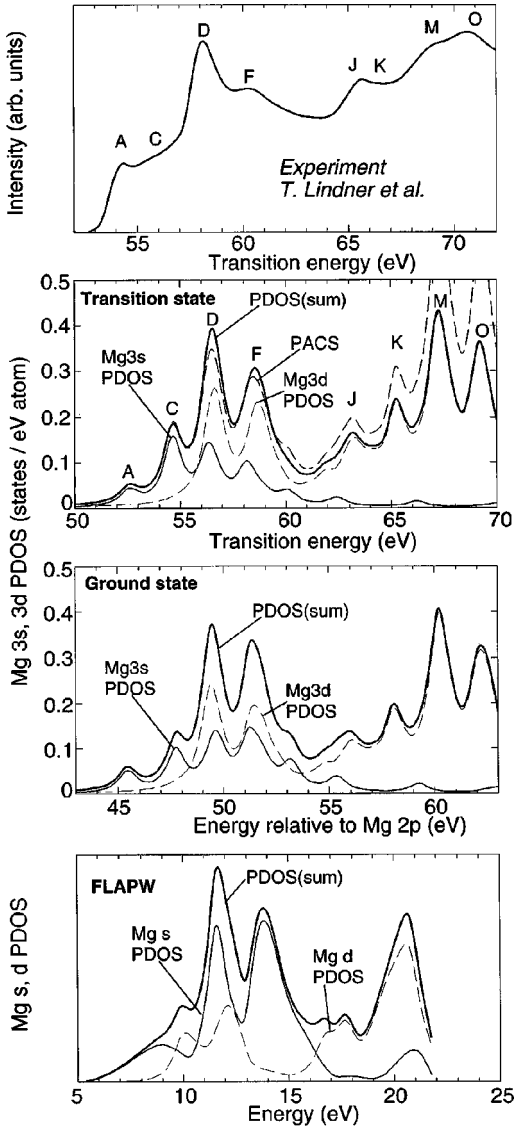

FIG. 2. (From top to bottom) Experimental Mg $L_{2,3}$-edge ELNES of MgO by Lindner *et al.* (Ref. 13). Theoretical Mg 3*s*,3*d* PDOS by a cluster $(Mg_{61}O_{62})^{2+}$ calculated for Slater's transition state and for the ground state. Mg *s* and *d* PDOS by the FLAPW band-structure calculation.

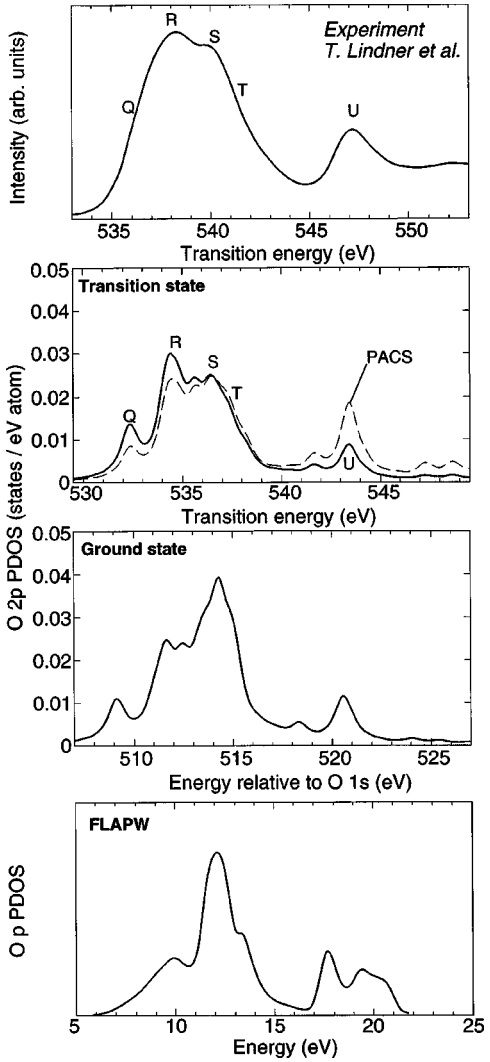

FIG. 3. (From top to bottom) Experimental O *K*-edge ELNES of MgO by Lindner *et al.* (Ref. 13). Theoretical O 2*p* PDOS by a cluster $(O_{63}Mg_{62})^{2-}$ calculated for Slater's transition state and for the ground state. O *p* PDOS by the FLAPW band-structure calculation.

butions of 3*s* and 3*d* states are not notably different in the case of the third-row elements, thereby making the relative contributions of the Mg 3*s* and 3*d* components to be close to unity.

The difference in the PDOS between the ground state and the transition state is much smaller than that found at the Mg *K* edge. The FLAPW result and the cluster result both at the ground states are in good agreement in the first 10 eV. The sum of PDOS's by Köstlmeier and Elsässer[8] also agrees with these results in this energy range. However, the allotments to PDOS's are different between the FLAPW and the cluster results. This may be ascribed to the different choice in the basis functions between two methods, since the comparison has been made merely for PDOS not for PACS. The detailed origin of the discrepancy has not been clarified yet.

Although the sums of Mg 3*s* and 3*d* PDOS's at the ground and the transition states are similar, subtle difference in the intensity of peaks *D* and *F* can be noted. The intensity ratio I_F/I_D, decreases when a half-filled core hole is included. The experimental spectrum shows much smaller I_F/I_D, implying that the core-hole effect to change the I_F/I_D is more significant than that evaluated by the transition-state calculation. A small peak denoted as *C* appears in the theoretical spectrum between peaks *A* and *D*. However, this may correspond to a broad plateau between peaks *A* and *D* in the experimental spectrum. Other than these differences in peak intensities and widths, the agreement between the experimental and theoretical spectrum by the cluster calculation for the transition state may be satisfactory. The absolute transition energy by the present calculation at the Mg L_{23} edge is different by approximately 2 eV with the ELNES and 1 eV with the NEXAFS. The difference between theory and experiment is as small as possible in terms of experimental errors.

C. O *K*-edge spectrum

The experimental ELNES by Lindner *et al.*[13] is compared in Fig. 3 with theoretical spectra in the same way as in pre-

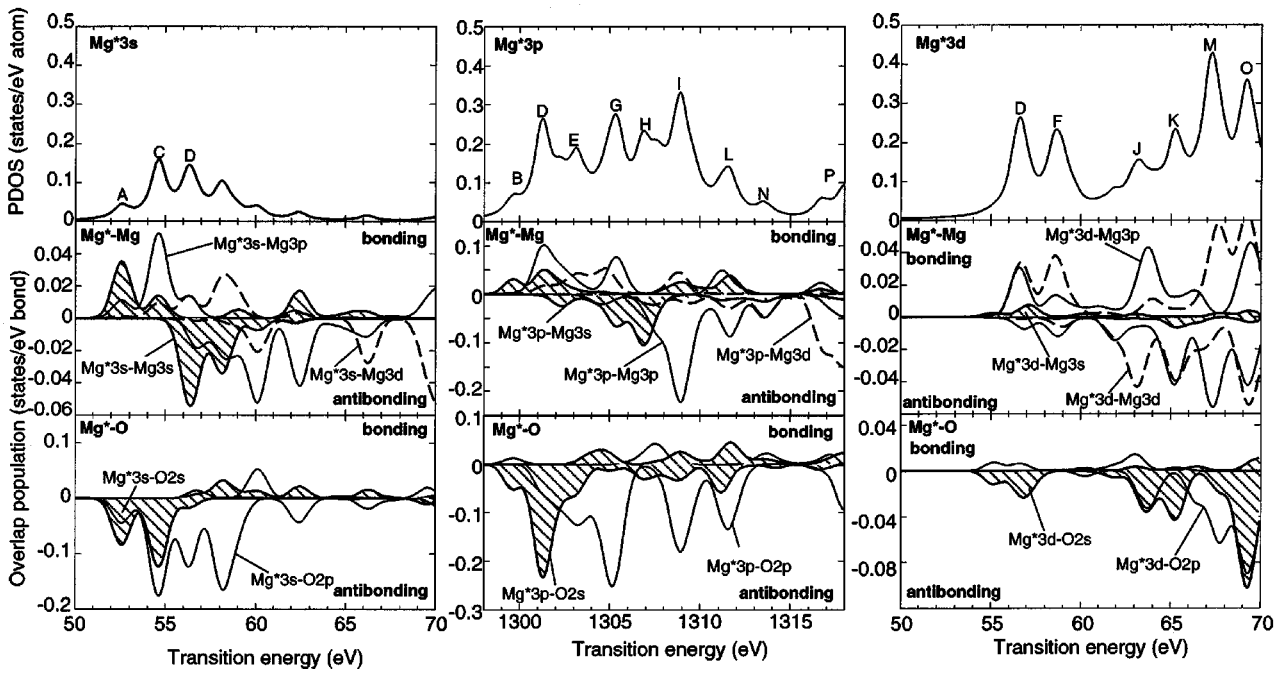

FIG. 4. Unoccupied PDOS of Mg* 3*s* (left), Mg* 3*p* (center), and Mg* 3*d* (right) by a cluster $(Mg_{63}O_{62})^{2+}$ for Slater's transition state, and their related overlap-population diagrams. Mg* denotes the core-hole Mg atom. In the overlap-population diagrams of Mg*-Mg (second row), the Mg*−Mg 3*s*, and Mg*−Mg 3*p* and Mg*−Mg 3*d* contributions are shown by the hatched area, solid curve, and broken curves, respectively. Because of the presence of the core hole, Mg* 3*s*−Mg 3*p* and Mg* 3*p*−Mg 3*s* are not the same, for example. In the overlap-population diagrams of Mg*-O (third row), Mg*−O 2*s* and Mg*−O 2*p* are shown by the hatched area and solid curve.

vious figures. For the calculation of the O *K* edge, a cluster composed of 125 atoms but centered on an oxygen atom is used. Since the oxygen components are minor near the bottom of the conduction band, we can first expect greater uncertainty of the theoretical spectra associated with the choice of the computational methods. However, at the ground state, agreement between results by the FLAPW and the cluster method are acceptable. Agreement between two band-structure results by the FLAPW and by Köstlmeier and Elsässer[8] is also very good. However, these ground-state results do not reproduce the experimental features, especially the intensity ratio of peaks *R* and *S*, I_R/I_S. This should also be ascribed to the core-hole effect. However, in contrast to the Mg edges, the absolute values of the O 2*p* PDOS at the core-hole atom are decreased especially around peaks *R* and *S* upon the localization. The strange-looking behavior can be understood when one recalls that oxygen is the minor component of the energy range of interest. When an O 1*s* core hole is made, the covalent interaction between Mg and O is weakened. This is qualitatively the same as the difference between Mg-O and Mg-F assuming the $Z+1$ effect.[12] The Mg-F bond is less covalent from the viewpoint of the electronegativity difference. The decrease in the covalent interaction should decrease the fraction of the oxygen components in the unoccupied band in metal oxides.

The absolute transition energy by the present calculation agrees with the experimental one with an error of approximately 3.5 eV (0.7% of the transition energy). Besides the agreement in the transition energy, the shape of the experimental spectrum is well reproduced. A small peak denoted by *Q* appears in our PDOS of the transition state. Although peak *Q* is not clearly seen in the experimental spectrum, we can assume its presence at the low-energy shoulder of the main peak.

D. Origin of peaks in Mg-edge spectra

In order to understand the origin of peaks from the viewpoint of interactions among atomic orbitals, overlap-population diagrams are systematically investigated. They are made by broadening the overlap populations defined by Eq. (3) using Gaussian functions of 1.0 eV FWHM. Figure 4 compares the PDOS of Mg orbitals and overlap-population diagrams of the corresponding components obtained by the large cluster for the transition state. The notation Mg* will be hereafter used in order to distinguish the core-hole Mg (Mg*) from its surrounding Mg atoms. The overlap population diagrams among Mg orbitals are shown together with those between Mg* and O orbitals. Although the overlap populations among Mg* and O orbitals are greater, they mainly exhibit an antibonding interaction.[18] On the other hand, the Mg*-Mg interactions display both bonding and antibonding interactions. The shape of the wave functions in the unoccupied band is therefore well characterized by the Mg*-Mg interaction. The shape of the overlap-population diagrams for Mg*-O interactions looks similar to the PDOS of the corresponding Mg orbital.

Most of the peaks that appear in the PDOS are found in the Mg*-Mg overlap-population diagrams. These peaks are denoted by letters from *A* to *P* in order of energy. Common notation is sometimes used for different PDOS's. For example, peak *D* appears in all three PDOS's. At the ground state, such common structures of the DOS can be simply explained by the hybridization of Mg *s*-*p*-*d* orbitals. Strictly speaking, the electronic structures of the Mg 1*s*−hole state and the Mg 2*p*−hole state are not directly comparable. As can be seen in Fig. 1, however, the presence of the core hole does not sensibly change the peak shape around peak *D*. We can therefore use the same notation, peak *D*, for different hole states.

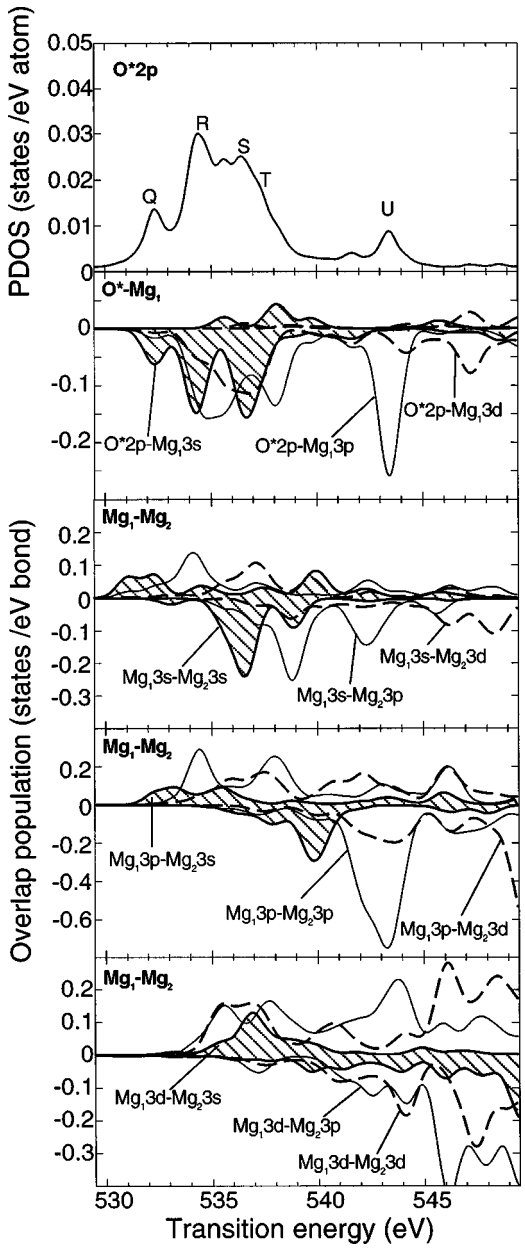

FIG. 5. (From top to bottom) Unoccupied PDOS of O* $2p$ by a cluster $(O_{63}Mg_{62})^{2-}$ for Slater's transition state, and overlap-population diagrams for O*-Mg_1 and Mg_1-Mg_2 interactions.

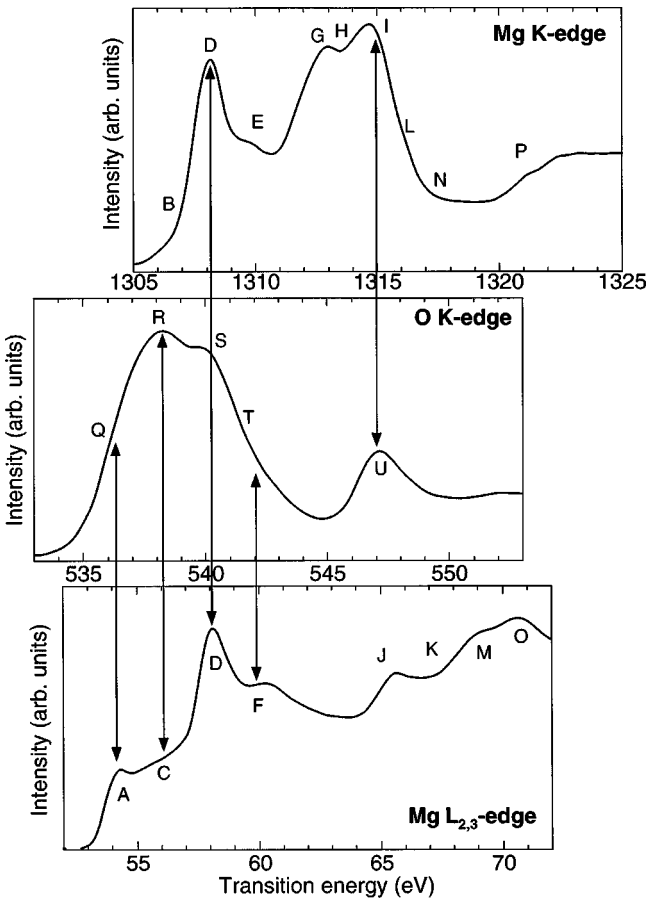

FIG. 6. Three experimental spectra by Lindner *et al.* (Ref. 13) aligned at features of the common origins.

Peaks A and D found in the Mg* $3s$ PDOS are different in the phase of the MO. Peak A corresponds to the bonding interaction for Mg* $3s-\mathrm{Mg}\,3s$. On the other hand, peak D represents the antibonding interaction. Peak C also originated from the Mg* $3s-\mathrm{Mg}\,3s$ bonding similar to peak A. However, a greater contribution of the Mg* $3s-\mathrm{Mg}\,3p$ bonding can be noted.

The peaks B/D and G/H in the Mg* $3p$ PDOS are similar. They are determined by the bonding and the antibonding interactions between Mg* $3p$ and Mg $3s$, although some bonding interaction of Mg* $3p-\mathrm{Mg}\,3p$ can be seen for peak D. The interactions between Mg* $3p$ and Mg $3p$ determine peaks D/G and $I/L/N$. The scale of the vertical axis shows that the magnitude of the overlap populations between Mg* $3p$ and the surrounding Mg orbitals are 2–3 times greater than those between Mg* $3s$ and other Mg orbitals. The antibonding interaction of Mg* $3p-\mathrm{Mg}^*\,3p$ for peak I is remarkably strong. This is the peak that contributes to the pronounced peak in the Mg $3p$ PDOS by the band-structure calculation (Fig. 1).

In the Mg* $3d$ PDOS, the Mg* $3d-\mathrm{Mg}\,3d$ interaction is bonding for the twin peak D/F. They are different in the Mg* $3d-\mathrm{Mg}\,3p$ interaction. Peaks located at energies higher than J originate from the Mg* $3d-\mathrm{Mg}\,3p$ and Mg* $3d-\mathrm{Mg}\,3d$ interactions. However, they are rather complicated. Peak energies are determined in these ways depending upon the atomic orbital compositions and the geometry of the MO.

E. Origin of peaks in the O *K*-edge spectrum

Figure 5 show the O* $2p$ PDOS and overlap-population diagrams for O*-Mg_1 and Mg_1-Mg_2, where Mg_1 is located at the first nearest neighbor of O* and Mg_2 is at the second nearest cation site. A calculation is made for the transition state using a cluster composed of 125 atoms. It should be noted that the cluster is centered with an O atom, which is different from that used in Fig. 4. Peaks that appear in the O* $2p$ PDOS are denoted by letters from Q to U. Both the O*-Mg_1 and Mg_1-Mg_2 interactions are responsible for these peaks. Regarding the O*-Mg_1 interaction, O* $2p-\mathrm{Mg}_1\,3s$ antibonding is important for peaks Q, R, and S, although O* $2p-\mathrm{Mg}_1\,3p$ antibonding also contributes for peaks R and S. The peaks T and U are mainly due to the O* $2p-\mathrm{Mg}_1\,3p$

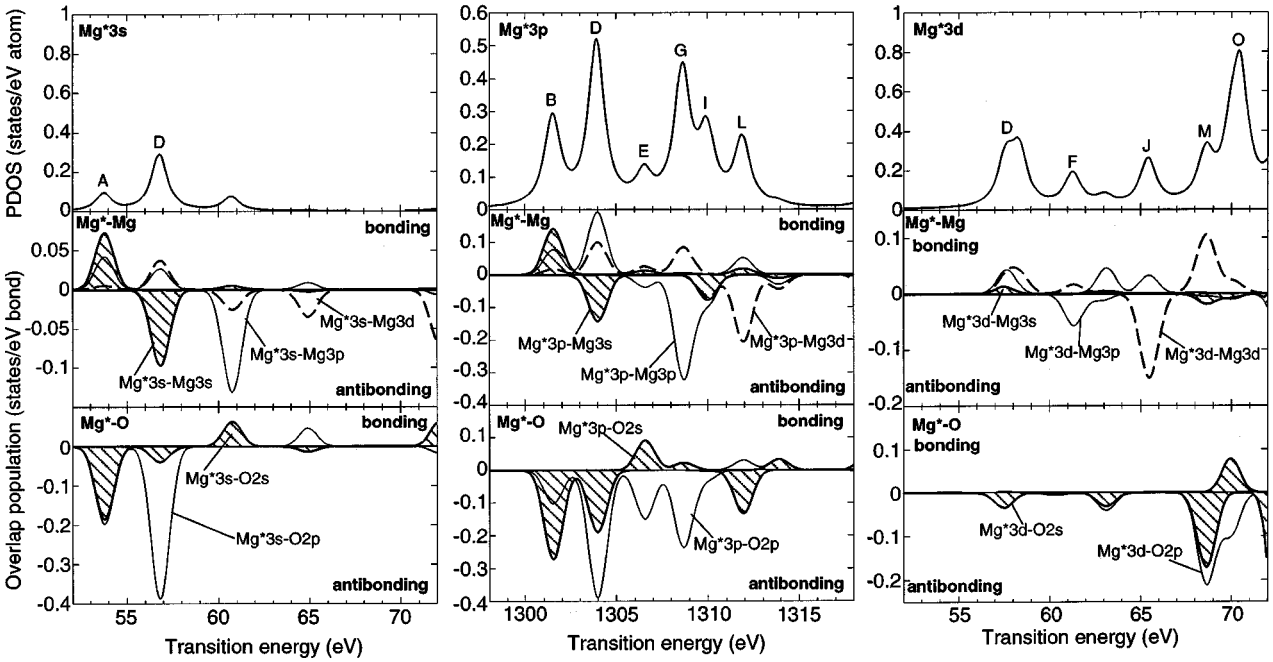

FIG. 7. Unoccupied PDOS of Mg* 3*s* (left), Mg* 3*p* (center), and Mg* 3*d* (right) by a cluster $(Mg_{13}O_{14})^{2-}$ for Slater's transition state, and their related overlap-population diagrams.

antibondings. The antibonding between O* 2*p* and Mg_1 3*d* determines peak *S* and other tiny peaks located at higher energies than peak *U*.

Concurrent to these O*-Mg_1 interactions, correlation between overlap population diagrams of the Mg_1-Mg_2 interaction and O* 2*p* PDOS can be noted. Peaks *Q* and *R* are found to correspond to the $Mg_1\,3s-Mg_2\,3s$ and $Mg_1\,3s-Mg_2\,3p$ bonding, respectively, which are similar to peaks *A* and *C*. Peaks *S* and *T* correspond to peaks *D* and *F*, respectively. A similarity between peak *U* and peak *I* can also be noted.

On the basis of this information, the experimental spectra at three edges may be aligned at some common features as shown in Fig. 6. As already mentioned, the three spectra are not necessarily well aligned because they suffer from different kinds of core-hole effects. However, the three experimental spectra are well aligned since the core-hole effects are not too significant to change the relative energies of peaks completely.

F. Comparison with smaller clusters

In our previous report,[7] we reported that the calculation using a small cluster of hexagonal BN exhibits better agreement with experiment as compared with that of a large cluster when the presence of the core hole is ignored. Moreover, we have experienced in a number of systems that calculations using small clusters qualitatively reproduce experimental ELNES and NEXAFS.[2–6] The agreement seems not to be accidental, since the calculation using a small cluster forces localization of the wave function even when the core hole is not included, thereby imitating core-hole effects. The use of a small cluster makes the interpretation of spectral features easy, which may be advantageous when one needs to understand the origin of spectral features qualitatively.

Figure 7 displays plots similar to Fig. 4 using a smaller cluster composed of 27 atoms and centered with a Mg atom. Calculations were made for the transition state. Peaks in the PDOS are denoted by letters in reference to the large cluster using overlap-population diagrams. It is true that some of fine structure is missing in the PDOS from the small cluster. Assignment of peaks with respect to the bonding states is not always the same. It should be due to an insufficient number of Mg atoms to describe the wave functions of the core-hole state. Wave functions are forced to localize too much in the small cluster. However, we would like to emphasize that major orbital interactions are included in the small cluster, thereby reproducing the major features of experimental spectra. This can be explained by the fact that the nearest-neighbor Mg-Mg interaction is already included in the small cluster. The Mg-Mg interactions determine the fine structure of the DOS. The result using the small cluster may be useful for qualitative arguments. In addition, the transition energies of the first peaks are in good agreement. Discussion of the absolute transition energies or chemical shifts can be sufficiently made using the small cluster.

IV. SUMMARY

A first-principles molecular orbital calculation using model clusters is made in order to reproduce and interpret ELNES and NEXAFS of MgO. Major results can be summarized as follows:

(1) PDOS's at the ground state by the present cluster method using a model cluster composed of 125 atoms and FLAPW are in good agreement. However, they do not reproduce the experimental ELNES and NEXAFS satisfactorily. Features in the experimental spectra are found to be reproduced only by the calculation for Slater's transition state, where a half-filled hole is put into a core orbital. This means a large supercell is required to reproduce the experimental spectra when one uses a band-structure method.

(2) The origin of peaks appearing in the experimental spectra are interpreted in terms of orbital interactions using overlap-population diagrams. Peaks that appear in the Mg-edge spectra are denoted by letters from *A* to *P* on the basis of the manner of Mg*-Mg interactions. Those in the O *K*-edge spectrum are denoted by *Q* to *U*. Both the O*-Mg_1 and Mg_1-Mg_2 interactions are responsible for these O *K*-edge peaks. As a result of those interpretation, some peaks in the spectra at different edges are pointed out to have common origins. Experimental spectra are aligned accordingly as shown in Fig. 6.

(3) The transition energies and qualitative features of experimental spectra are found to be reproduced using a smaller cluster composed of 27 atoms, although some of fine structure is missing. The dual reasons are (a) the smaller cluster includes the nearest-neighbor Mg-Mg interactions that determine the qualitative features, and (b) the calculation using a small cluster forces localization of the wave function, thereby qualitatively simulating the core-hole effects.

ACKNOWLEDGMENTS

We thank S. Köstlmeier and C. Elsässer for showing us Ref. 8 prior to publication, and S. Nagano for technical assistance. This work was supported by a Grant-in-Aid for General Scientific Research from Ministry of Education, Sports, Science and Culture of Japan.

[1] *Unoccupied Electronic States*, edited by J. C. Fuggle and J. E. Inglesfield (Springer-Verlag, Berlin, 1992).
[2] I. Tanaka, J. Kawai, and H. Adachi, Solid State Commun. **93**, 533 (1995).
[3] I. Tanaka, T. Nakajima, J. Kawai, and H. Adachi, H. Gu, and M. Rühle, Philos. Mag. Lett. **75**, 21 (1997).
[4] I. Tanaka and H. Adachi, Phys. Rev. B **54**, 4604 (1996).
[5] I. Tanaka and H. Adachi, J. Phys. D **29**, 1725 (1996).
[6] H. Kanda, M. Yoshiya, F. Oba, K. Ogasawara, H. Adachi, and I. Tanaka, Phys. Rev. B **58**, 9693 (1998).
[7] I. Tanaka, H. Araki, M. Yoshiya, T. Mizoguchi, K. Ogasawara, and H. Adachi, Phys. Rev. B **60**, 4944 (1999).
[8] S. Köstlmeier and C. Elsässer (unpublished).
[9] D. E. Ellis, H. Adachi, and F. W. Averill, Surf. Sci. **58**, 497 (1976).
[10] H. Adachi, M. Tsukada, and C. Satoko, J. Phys. Soc. Jpn. **45**, 875 (1978).
[11] J. C. Slater, *Quantum Theory of Molecules and Solids* (McGraw-Hill, New York, 1974).
[12] T. Fujikawa, J. Phys. Soc. Jpn. **52**, 4001 (1983).
[13] T. Lindner, H. Sauer, W. Engel, and K. Kambe, Phys. Rev. B **33**, 22 (1986).
[14] The FLAPW calculation was done by ourselves using a program code WIEN97 [P. Blaha, K. Schwarz and J. Luitz, Vienna University of Technology, 1997. This is an improved and updated version of the original copyrighted WIEN code, which was published by P. Blaha, K. Schwarz, P. Sorantin, and S. B. Trickey, Comput. Phys. Commun. 59, 399(1990)].
[15] W. L. O'Brien, J. Jia, Q.-Y. Dong, T. A. Callcott, D. R. Mueller, D. L. Ederer, and C.-C. Kao, Phys. Rev. B **47**, 15 482 (1993).
[16] J. Chaboy, Solid State Commun. **99**, 877 (1996).
[17] H. Ebert, J. Stöhr, S. S. P. Parkin, M. Samant, and A. Nelsson, Phys. Rev. B **53**, 16 067 (1996).
[18] The in-phase and the out-of-phase interactions correspond to bonding and antibonding interactions only when the orbitals are occupied. However, we use ''bonding'' and ''antibonding'' for unoccupied orbitals for simplicity.